Energy Transfer between Polyatomic Molecules. 3. Energy Transfer Quantities and Probability Density Functions in Self-Collisions of Benzene, Toluene, *p*-Xylene and Azulene†

V. Bernshtein and I. Oref*

Department of Chemistry, Technion-Israel institute of Technology, Haifa 32000, Israel

Received: October 2, 2005; In Final Form: January 5, 2006

This paper is the third and last in a series of papers that deal with collisional energy transfer, CET, between aromatic polyatomic molecules. Paper 1 of this series (*J. Phys. Chem. B* **2005**, *109*, 8310) reports on the mechanism and quantities of CET between an excited benzene and cold benzene and Ar bath. Paper 2 in the series (*J. Phys. Chem.*, in press) discusses CET between excited toluene, *p*-xylene and azulene with cold benzene and Ar and CET between excited benzene colliding with cold toluene, *p*-xylene and azulene. The present work reports on CET in self-collisions of benzene, toluene, *p*-xylene and azulene. Two modes of excitation are considered, identical excitation energies and identical vibrational temperatures for all four molecules. It compares the present results with those of papers 1 and 2 and reports new findings on average vibrational, rotational, and translational energy, $\langle\Delta E\rangle$, transferred in a single collision. CET takes place mainly via vibration to vibration energy transfer. The effect of internal rotors on CET is discussed and CET quantities are reported as a function of temperature and excitation energy. It is found that the temperature dependence of CET quantities is unexpected, resembling a parabolic function. The density of vibrational states is reported and its effect on CET is discussed. Energy transfer probability density functions, $P(E,E')$, for various collision pairs are reported and it is shown that the shape of the curves is convex at low temperatures and can be concave at high temperatures. There is a large supercollision tail at the down wing of $P(E,E')$. The mechanisms of CET are short, impulsive collisions and long-lived chattering collisions where energy is transferred in a sequence of short internal encounters during the lifetime of the collision complex. The collision complex lifetimes as a function of temperature are reported. It is shown that dynamical effects control CET. A comparison is made with experimental results and it is shown that good agreement is obtained.

Introduction

This is the third paper in a series that deals with collisional energy transfer, CET, between aromatic polyatomic molecules. Understanding polyatomic−polyatomic, PP, collisions is necessary to understand combustion, atmospheric, astrophysical and astrochemical reactions; all involve thermal, photophysical and photochemical processes.[1] Despite the ubiquity of the above chemical transformation, little is known about the detail mechanism of the energy exchange. Questions such as, how is energy transferred in the collision process and how does it depend on internal factors: size, normal modes frequencies, internal rotors and on external conditions of temperature and internal excitation are still partially unanswered and it is the purpose of this series of papers to shed light on some of them. The lack of information on CET in PP is not due to lack of interest but more to experimental difficulties[2] that make it hard to obtain ample data readily available for interpretation. The first paper in the series,[3] paper 1, dealt with benzene−benzene, B−B, collisions and provided insight into the mechanism of energy transfer. Paper[4] 2 expends previous work reported in paper 1 on B−B collisions and explores collisions of excited toluene, T*, *p*-xylene, pX*, and azulene, AZ*, with cold benzene bath and B* collisions with T, pX, and AZ bath. It also presents results and discusses collisions between T*, pX*, and AZ* and Ar and makes a comparison between polyatomic and monatomic colliders. The effect of internal rotation on CET was studied by comparing T and pX to B and AZ. pX and AZ are structurally different but have the same number of normal modes and hence very similar vibrational−rotational temperatures, which facilitates a comparison between the CET quantities of the two molecules. Also the effect of identical vibrational−rotational temperatures in all four molecules on CET was studied.

The major findings of the two papers are (a) The major channel for energy transfer in PP collisions is vibration to vibration, V−V, energy transfer, assisted by rotations and translation. (b) A mechanism for obtaining high values of $\langle\Delta E\rangle$, in addition to short impulsive collisions, is chattering collisions where energy is transferred in a sequence of short internal encounters during the lifetime of the collision complex. (c) Supercollisions can occur in PP by multiple encounters during the lifetime of the collision complex. (d) The shape of the down-collisions wing of the probability density function $P(E,E')$ in PP collisions is convex at low temperatures and becomes concave at higher temperatures. (e) The value of total average energy transferred per collision, $\langle\Delta E\rangle_a$, in PP collisions is much larger than that in a polyatomic−monatomic collision due to the fact that there is an extra V−V channel that is absent in the latter. (f) Freezing rotations enhances CET in PP because it facilitates the formation of a collision complex. (g) The gateway modes for CET are the low-frequency out-of-plane, OOP, modes of the excited polyatomic molecule. (h) Very small net overall rotational energy, $\langle\Delta E_R\rangle_a$, is transferred during the CET but the average values of the up and down CET, $\langle\Delta E_R\rangle_{u,d}$ are large,

† Part of the "Chava Lifshitz Memorial Issue".

* Corresponding author. E-mail: chroref@technion.ac.il.

10.1021/jp055612q CCC: $33.50
Published on Web 02/04/2006

which indicate active participation of rotations in the energy transfer process. (i) Overall translational energy transfer is small. However, the values of the average up and down transfer are fairly large, 100−250 cm^{-1} depending on the temperature. (j) Internal rotations in the excited molecule hinder energy exchange whereas in the bath molecule they do not because the internal rotors are not excited. (k) In the temperature range 200−600 K, energy transfer at low temperatures is more efficient than at high temperatures where $\langle\Delta E\rangle_a$ levels off. (l) Low-frequency modes enhance energy transfer. Thus, azulene with the same number of normal modes as *p*-xylene but with modes of lower frequencies and without internal rotations is much more efficient in transferring energy to benzene bath molecules. (m) Energy transfer depends on the initial translational energy at lower values and reaches a plateau at higher values. (n) Vibrational temperatures affect energy transfer. In a series of polyatomic molecules of different sizes and identical vibrational temperatures, i.e., different excitation energies, the largest values of $\langle\Delta E\rangle_a$ occur in the largest molecules with the lowest frequency modes. (o) The collision lifetime is long at low temperatures. This enables many chattering collisions to take place and, therefore, this is one of the main reasons for the large values of $\langle\Delta E\rangle_a$ at low temperatures.

As indicated above, CET is not symmetric. That is to say, $\langle\Delta E\rangle_a$ for collisions of T*, pX*, and AZ* with B is less effective than B* colliding with T, pX, and AZ because the latter have lower normal-mode frequencies than B and the unexcited internal rotors in T and pX do not hinder energy transfer. It is important, therefore, to study CET in self-collisions where the excited and bath molecules are identical, which means, of course, matching donor and acceptor frequencies. As will be seen, there are indeed, basic differences between regular and self-collisions. In addition, CET between B*, T*, pX*, and AZ* and Ar is studied and a comparison is made between CET in aromatic polyatomic−polyatomic and aromatic polyatomic−monatomic collisions. The results will be compared with experiments on CET in self-collisions wherever they are available.

Theory

Because it is the third paper in a series that uses the same computational technology, it is superfluous to repeat the details here. Therefore, only the bare minimum is discussed and for additional details the reader is referred to paper 1 and refs 5 and 6. The classical equations of motion that describe the relative motion of the colliding pair include the inter- and intramolecular potentials. The intramolecular potential includes all the normal mode contributions, stretching, bending, torsion and wagging.[7,8] The calculated and experimental normal modes frequencies are given in Appendix IV of paper 2. The parameters of the pairwise intermolecular Lennard-Jones (LJ) potential of B−B, which are reported in paper 1, were used for the rest of the aromatic molecules in the series using Lim's method.[9,10] A table of experimental and calculated values of σ and ϵ together with the pairwise parameters σ_{ij} and ϵ_{ij} are presented in Appendix I and in Appendix II of paper 2.

The equations of motion were integrated by using a modified computer program Venus.[11] The initial relative translational and rotational energies were chosen from the appropriate thermal distributions. The initial vibrational energy was assigned in two ways. In one, a constant photon energy of 40 700 cm^{-1} was assigned to all molecules and the thermal energy at each temperature was added to it. In this case the average energy per mode in molecules of different sizes will be different, which might affect the values of the various $\langle\Delta E\rangle$ quantities. A unifying physical property is the vibrational temperature, T_V. After a molecule absorbs a photon, fast internal conversion occurs[12] and the molecule attains a microcanonical vibrational temperature. Therefore, all molecules were assigned identical T_V, which was the T_V of excited benzene and which was calculated by the use of eq 1 of paper 2. Of the four molecules studied, three have different numbers of normal modes, and therefore, to have identical T_V's, different values of excitation energy were used. A table of vibrational temperatures and internal energies for all four molecules at the temperatures studied is given in Appendix III of paper 2. The initial impact parameter was chosen randomly from values between 0 and its maximum value, b_m. The value of the maximum impact parameter was determined separately for each molecule.[5,6]

The collision duration was determined by monitoring the beginning and the end of each collision by the forward and backward sensing (FOBS) method.[5,6,13] In the FOBS method a collision is defined by a change ϵ in the internal energy of the excited molecule in a time interval Δt. After careful and exhaustive study, the ratio $\epsilon/\Delta t$ was taken to be 0.35 cm^{-1}/fs. Approximately 50 000 trajectories were used for each set of initial conditions. A large number of trajectories was used to provide a good statistical sampling in the binning process. The FOBS method was also used in identifying effective collisions among the total elastic and inelastic collisions.

The average energy transferred quantities were calculated by the following equation

$$\langle\Delta E_X\rangle_Y = \sum_i^{N_j} \Delta E_X/N_j \qquad (1)$$

Where X can be V, R or T. ΔE without X indicate "all" quantities. Y indicates up, down or all quantities. N_j indicates the number of effective trajectories as determined by FOBS. For example, in a given set of trajectories, in calculating $\langle\Delta E_V\rangle_d$, the effective N_j is the number of all trajectories in which the molecule lost vibrational energy. The value of N_j changes for each quantity; therefore, N_j for $\langle\Delta E_V\rangle_d$ is different from that for $\langle\Delta E_T\rangle_d$ in the same set of trajectories. When we compare our results with experimental ones, we always use the total number of collisions, effective or not. The disadvantage of using the total number of trajectories instead of effective ones to study the mechanism of CET is a good number of them describe large-impact parameter elastic collisions that do not transfer energy at all. By mixing elastic and inelastic collisions, we get average CET quantities that are smaller than the actual average energy transferred in a collision. Therefore, we report results both for effective and total number of trajectories. The former is used to draw mechanistic conclusions and the latter for comparison with experimental results and other computational work reported in the literature.

In comparing the present results with experiments, we used the following expressions:

$$\langle\Delta E\rangle = \langle\Delta E\rangle_{trj}\frac{{b_m}^2}{{b_{ref}}^2(\text{exp})} \qquad (2)$$

where $b_{ref} = (\sigma_{LJ}{}^2\Omega^{(2,2)*})^{1/2}$ and $\langle\Delta E\rangle_{trj} = \sum_{i=1}^{N_{trj}}\Delta E_i/N_{trj}$, b_m is the maximum impact parameter, $\Omega^{(2,2)*}$ is the collision integral and N_{trj} is the total number of trajectories. The collision integral was determined from the equation[14] $\Omega^{(2,2)*} = [(a + b\log(kT/\epsilon)]^{-1}$. However, between 200 and 700 K the collision integral is given by Ross[15] $\Omega^{(2,2)*} = a(kT/\epsilon)^{-1/2}$ with an accuracy of

<0.7%. What these equations tell us is the number of collisions in the range 200−700 K is independent of the temperature and above it only weakly dependent on the temperature. This means that the dependence of the experimental values of the CET parameters on temperature is a function of the CET mechanism and is not due to a change in the number of collision with temperature.

Below we report on collisional energy transfer in self-collisions of benzene, toluene, *p*-xylene, and azulene and in collisions between excited toluene, *p*-xylene, and azulene with cold benzene bath and excited benzene collisions with toluene, *p*-xylene, and azulene. We also report and discuss collisions between excited toluene, *p*-xylene, and azulene and Ar bath and a comparison is made between polyatomic and monatomic colliders.

Results and Discussion

As will be seen in the following pages, even in the four similar molecules used in the present study, B, T, pX, and AZ, it is hard to generalize and to find simple rules for CET. The molecular details dictate the energy transfer mechanism and thus the outcome of a collisional event with identical excitation energies and vibrational temperatures. One would expect self-collisions, because of resonance energy transfer, to be more efficient than collisions between similar, but not identical, colliders, which is true in some cases and not in others and for good reasons that are discussed in the following sections.

Average Energy Transferred in a Collision. The amount of average energy transferred per collision is shown in Table 1 and in Figure 1. The CET results of self-collisions are given in Table 1 for temperatures 300, 600, 1000, and 1500 K. The values are based on effective collisions as defined by FOBS, that is to say, all collisions in which there is, at least, a minimal interaction between the colliding pair. Examination of Figure 1 shows that $\langle \Delta E \rangle_d$ for self-collisions behaves differently at low and at high temperatures. There is a crossover between B and pX. At low temperatures CET in pX*−pX and AZ*−AZ is more efficient than for T*−T and B*−B whereas at high temperatures self-collisions of B and AZ are more efficient than those of T and pX. This temperature dependence was explained in paper 2 for mixed collisions, B* with T, pX, and AZ and T*, pX*, and AZ* with B, in the following way: at low temperatures the internal rotors of T and pX as bath gas are not excited and are not, therefore, in the way of forming a long-lived collision complex or inhibiting energy transfer. The two molecules, pX and AZ, have low lying vibrations that are efficient gateway modes for CET. T with its unexcited internal rotor is as efficient as B. Both have higher frequency gateway modes than pX and AZ, and therefore, they are less efficient. At high temperatures, above 600 K, the mechanism for CET changes and the collisions become impulsive. The internal rotors of the bath are excited and are in the way of CET. Thus B and AZ, without active internal rotors, are more efficient than T and pX. Around the transition temperature of 400 K, where the curves cross, the situation is complicated as transition is made from low to high-temperature behavior. In addition, as will be discussed later on, a change from low to high temperatures causes a change in the relative kinetic energy of the colliding pairs which changes the mechanism from more complex forming collisions to more impulsive ones. Also, the overall rotations increase with temperature and affect the CET. The high values of $\langle \Delta E \rangle_d$ at low temperatures are caused by multiple encounters during the lifetime of the collision complex, chattering collisions, whereas the high values at high temperatures are caused by strong, impulsive collisions.

TABLE 1: Energy Transfer Quantities in Self Collisions of Various Collision Pairs[a]

	hot molecule				cold bath molecule			
	B*−B	T*−T	pX*−pX	AZ*−AZ	B*−B	T*−T	pX*−pX	AZ*−AZ
				$T = 300$ K				
$\langle \Delta E \rangle_a$	−755	−753	−823	−1176	737	737	812	1122
$\langle \Delta E \rangle_d$	−889	−877	−959	−1308	−53	−57	−57	−63
$\langle \Delta E \rangle_u$	55	60	70	61	869	853	932	1252
$\langle \Delta E_V \rangle_a$	−767	−762	−825	−1193	731	732	817	1110
$\langle \Delta E_V \rangle_d$	−874	−872	−943	−1310	−13	−35	−28	−37
$\langle \Delta E_V \rangle_u$	27	51	46	42	815	822	907	1219
$\langle \Delta E_R \rangle_a$	12	9	2	18	7	4	−6	13
$\langle \Delta E_R \rangle_d$	−126	−116	−124	−124	−126	−120	−127	−128
$\langle \Delta E_R \rangle_u$	144	128	126	147	136	126	128	143
$\langle \Delta E^{H+C_T} \rangle_a$	18	16	11	52				
$\langle \Delta E^{H+C_T} \rangle_d$	−136	−154	−165	−163				
$\langle \Delta E^{H+C_T} \rangle_u$	157	178	181	230				
$\langle \tau_{coll} \rangle_a$	2.23	2.61	3.18	3.58	2.23	2.61	3.18	3.58
$\langle \tau_{coll} \rangle_d$	2.39	2.79	3.41	3.79	1.27	1.38	1.54	1.64
$\langle \tau_{coll} \rangle_u$	1.29	1.41	1.63	1.63	2.39	2.79	3.41	3.79
				$T = 600$ K				
$\langle \Delta E \rangle_a$	−775	−679	−670	−946	756	691	689	919
$\langle \Delta E \rangle_d$	−1027	−919	−917	−1202	−115	−124	−117	−135
$\langle \Delta E \rangle_u$	106	135	143	136	1012	908	914	1166
$\langle \Delta E_V \rangle_a$	−781	−671	−655	−947	754	710	723	920
$\langle \Delta E_V \rangle_d$	−1005	−899	−869	−1178	−44	−77	−70	−95
$\langle \Delta E_V \rangle_u$	71	158	109	117	963	878	896	1130
$\langle \Delta E_R \rangle_a$	6	−7	−15	1	1	−19	−34	−2
$\langle \Delta E_R \rangle_d$	−212	−215	−196	−206	−219	−205	−209	−213
$\langle \Delta E_R \rangle_u$	222	211	177	209	215	186	176	204
$\langle \Delta E^{H+C_T} \rangle_a$	19	−13	−20	27				
$\langle \Delta E^{H+C_T} \rangle_d$	−229	−268	−266	−271				
$\langle \Delta E^{H+C_T} \rangle_u$	248	250	252	309				
$\langle \tau_{coll} \rangle_a$	1.32	1.52	1.82	2.01	1.32	1.52	1.82	2.01
$\langle \tau_{coll} \rangle_d$	1.40	1.64	1.97	2.15	1.05	1.11	1.26	1.41
$\langle \tau_{coll} \rangle_u$	1.06	1.13	1.30	1.42	1.40	1.63	1.97	2.16
				$T = 1000$ K				
$\langle \Delta E \rangle_a$	−840	−709	−663	−937	−833	−741	−707	−922
$\langle \Delta E \rangle_d$	−1270	−1136	−1083	−1390	220	242	238	279
$\langle \Delta E \rangle_u$	220	274	283	284	−1258	−1144	−1100	−1373
$\langle \Delta E_V \rangle_a$	−849	−690	−633	−931	−831	−774	−757	−938
$\langle \Delta E_V \rangle_d$	−1216	−1061	−1002	−1362	123	185	167	219
$\langle \Delta E_V \rangle_u$	163	246	248	261	−1176	−1109	−1079	−1345
$\langle \Delta E_R \rangle_a$	9	−19	−31	−6	−2	33	49	17
$\langle \Delta E_R \rangle_d$	−316	−281	−290	−299	313	292	301	311
$\langle \Delta E_R \rangle_u$	326	253	242	289	−316	−252	−240	−283
$\langle \Delta E^{H+C_T} \rangle_a$	7	−33	−45	14				
$\langle \Delta E^{H+C_T} \rangle_d$	−337	−386	−398	−399				
$\langle \Delta E^{H+C_T} \rangle_u$	348	344	347	425				
$\langle \tau_{coll} \rangle_a$	0.97	1.09	1.28	1.42	0.97	1.09	1.28	1.42
$\langle \tau_{coll} \rangle_d$	1.02	1.16	1.37	1.51	0.86	0.93	1.08	1.20
$\langle \tau_{coll} \rangle_u$	0.87	0.93	1.10	1.20	1.02	1.15	1.37	1.50
				$T = 1500$ K				
$\langle \Delta E \rangle_a$	−924	−793	−768	−990	−906	−830	−817	−980
$\langle \Delta E \rangle_d$	−1575	−1477	−1417	−1720	362	432	407	492
$\langle \Delta E \rangle_u$	369	456	454	498	−1558	−1473	−1431	−1716
$\langle \Delta E_V \rangle_a$	−931	−768	−725	−977	−906	−879	−878	−1008
$\langle \Delta E_V \rangle_d$	−1516	−1362	−1303	−1667	257	352	319	427
$\langle \Delta E_V \rangle_u$	318	446	431	471	−1442	−1446	−1428	−1690
$\langle \Delta E_R \rangle_a$	7	−24	−43	−14	0	49	61	28
$\langle \Delta E_R \rangle_d$	−442	−395	−407	−410	422	402	407	423
$\langle \Delta E_R \rangle_u$	453	341	329	388	−422	−337	−315	−381
$\langle \Delta E^{H+C_T} \rangle_a$	18	−38	−50	10				
$\langle \Delta E^{H+C_T} \rangle_d$	−446	−528	−527	−534				
$\langle \Delta E^{H+C_T} \rangle_u$	465	461	472	564				
$\langle \tau_{coll} \rangle_a$	0.77	0.88	1.03	1.14	0.77	0.88	1.03	1.14
$\langle \tau_{coll} \rangle_d$	0.80	0.90	1.08	1.18	0.73	0.83	0.92	1.04
$\langle \tau_{coll} \rangle_u$	0.72	0.82	0.93	1.05	0.79	0.90	1.08	1.19

[a] $\langle \Delta E \rangle$ in units of cm^{-1} and $\langle \tau \rangle$ in ps. Excitation energy 40 700 cm^{-1}.

What happens when self-collisions are replaced with mixed collisions? Here, the nature of the bath molecule dictates the behavior. If B is the bath, then, as can be seen from Table 1,

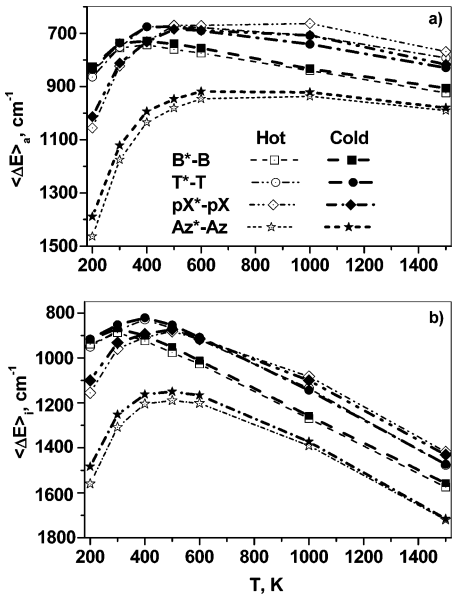

Figure 1. Absolute values of $\langle\Delta E\rangle$ as a function of temperature for self-collisions. $\langle\Delta E\rangle$ is negative for the hot molecule and positive for the cold molecule. (a) is for all collisions and (b) i indicates down collisions of the hot molecule and up collisions of the cold molecules. The excitation energy is 40700 cm^{-1} and the FOBS value is 0.35 cm^{-1} fs^{-1}. The decreasing numbers on the *y* coordinate are to facilitate comparison with previous work.[4]

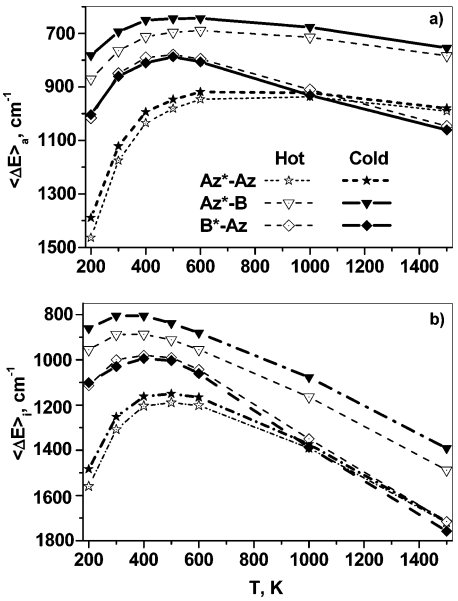

Figure 2. Absolute values of $\langle\Delta E\rangle$ as a function of temperature for the collision pair azulene-benzene. $\langle\Delta E\rangle$ is negative for the hot molecule and positive for the cold molecule. (a) is for all collisions and (b) i indicates down collisions of the hot molecule and up collisions of the cold molecules. Note the different behavior of the pair under different excitation conditions. The excitation energy is 40700 cm^{-1} and the FOBS value is 0.35 cm^{-1} fs^{-1}. The decreasing numbers on the *y* coordinate are to facilitate comparison with previous work.[4]

$\langle\Delta E\rangle_d$ in T*−B, pX*−B, and AZ*−B collisions is much lower than its vales in self-collisions of these molecules. B is a rigid molecule with fairly high normal-mode frequencies and is an inefficient collider compared with the other three molecules. This is supported by examining what happens in collisions of B* with the other three molecules as bath. They are as efficient, if not more so, than self-collisions of B. They are efficient because they have low lying modes and a larger intermolecular potential, which is a function of the size of the molecule, and, in addition, the internal rotors of T and pX are unexcited, all contributing to efficient energy transfer. The point is illustrated in Figure 2 where $\langle\Delta E\rangle_d$ is plotted vs temperature for collisions of three pairs of AZ*−AZ, AZ*−B, and B*−AZ. As can be seen, AZ*−B collisions are less efficient than B*−AZ collisions because AZ as bath is more efficient than B, AZ having lower normal-mode frequencies than B. In addition, there is probably resonance energy transfer that should be considered in self-collisions. The conclusion thus far is: there are no simple rules or predictions for CET and that pX can be much more efficient than B at low temperatures and the reverse will happen at high temperatures where B is much more efficient than pX. The temperature dependence is complex and cannot be represented by simple power as is often done.

For comparison, the temperature dependence of Ar colliding with the four molecules is different than that of polyatomic−polyatomic collisions and given in Figure 3. Although $\langle\Delta E\rangle_a$ is almost independent of the temperature the values of $\langle\Delta E\rangle_{u,d}$ are strongly and linearly dependent on temperature. This is true not only for $\langle\Delta E\rangle_{u,d}$ which describe the vibrational rotational change in the hot molecule but also to $\langle\Delta E_V\rangle_{u,d}$, which describes the net vibrational energy change in the hot molecule. The values of $\langle\Delta E_V\rangle_{u,d}$, however, are smaller than the values of $\langle\Delta E\rangle_{u,d}$, indicating the large contribution of rotations to the values of $\langle\Delta E\rangle_{u,d}$. For AZ−Ar collisions, for example, $\langle\Delta E\rangle_d$ in the temperature range 200−600 K can be expressed by $\langle\Delta E\rangle_d = -(90 + 0.45T)$. This is different than the temperature dependence in AZ−Xe collisions reported by Clarke[16] et al. to be

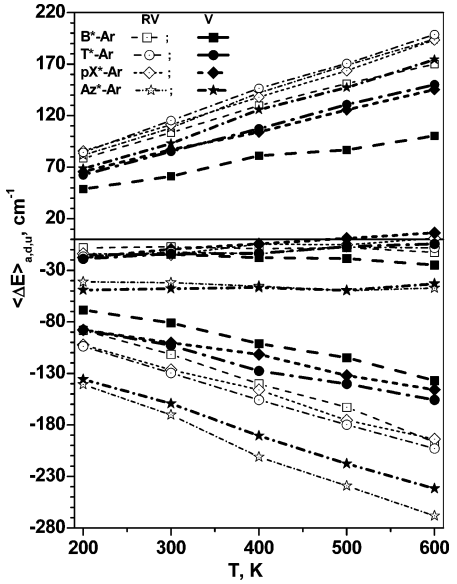

Figure 3. Value of $\langle\Delta E\rangle$ for polyatomic−Ar collisions as a function of temperature. RV indicates the internal vibrational/rotational energy and V the internal vibrational energy of the hot molecules. The excitation energy is 40700 cm^{-1} and the FOBS value is 0.35 cm^{-1} fs^{-1}.

$\langle\Delta E\rangle_d \propto T^{0.23}$. Of course, Xe is heavier and the van der Waals interactions are stronger, which may affect the temperature dependence.

Details of Energy Transfer: Vibrational, Rotational, and Translational. How is the energy being transferred from a hot to a cold molecule? Figures 1, 2, and 4−7 provide clues to the channels by which energy is being transferred from hot to cold molecule. In Figure 1 the absolute values of $\langle\Delta E\rangle_a$ and $\langle\Delta E\rangle_d$ of the hot molecule and $\langle\Delta E\rangle_u$ of the cold molecule are plotted as a function of temperature. As can be seen, the vibrational rotational energy lost by the hot molecule is gained by the cold

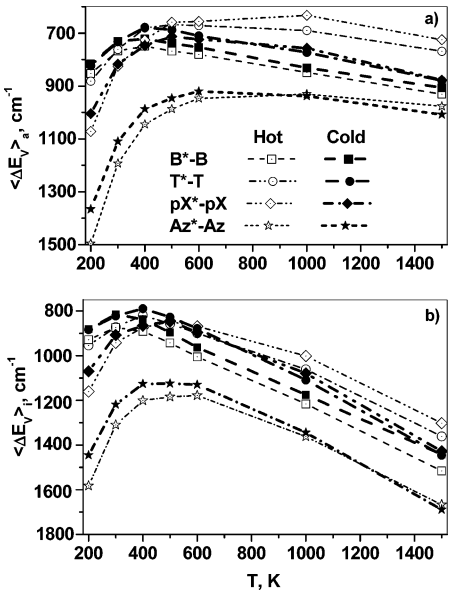

Figure 4. Absolute value of $\langle \Delta E_V \rangle$ for the hot and cold collision pair as a function of temperature. $\langle \Delta E_V \rangle$ is negative for the hot molecule and positive for the cold molecule. Note the efficient V−V transfer between hot and cold molecules. (a) is for all collisions and (b) i indicates down collisions of the hot molecule and up collisions of the cold molecules. The excitation energy is 40700 cm^{-1} and the FOBS value is 0.35 cm^{-1} fs^{-1}. The decreasing numbers on the *y* coordinate are to facilitate comparison with previous work.[4]

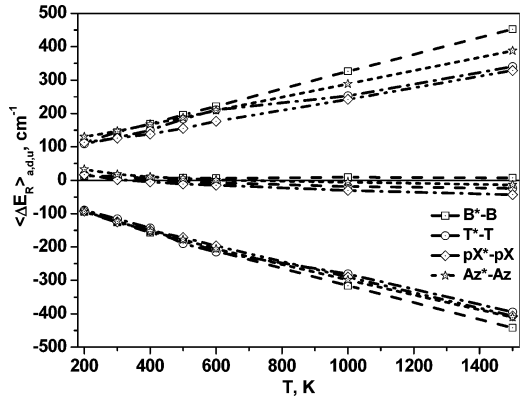

Figure 5. Up, down, and all value of average rotational energy transferred $\langle \Delta E_R \rangle$ as a function of temperature. The excitation energy is 40700 cm^{-1} and the FOBS value is 0.35 cm^{-1} fs^{-1}.

one, the small difference between the hot and the cold line is due to vibration/rotation to translation, V/R → T, energy exchange. This can also be seen in Figure 4 where $\langle \Delta E_V \rangle_a$ and $\langle \Delta E_V \rangle_d$ of the hot molecule and $\langle \Delta E_V \rangle_u$ of the cold molecule are given as a function of temperature. As can be seen, whatever vibrational temperature is lost by the hot molecule is gained by the cold molecule. The small difference in $\langle \Delta E_V \rangle$ between hot and cold molecules at low temperatures is due to V/R → T energy transfer. Careful examination of the graphs shows that there is a temperature range around 400−500 K where an inversion occurs and the cold molecule gains slightly more vibrational energy than the hot molecule loses. This probably comes about from the fact that the system is not canonical and the initial conditions of the cold molecule are an average thermal energy instead of a distribution.

Figure 5 shows the values of $\langle \Delta E_R \rangle_{a,u,d}$ as a function of temperature and Figure 6 shows the values of $\langle \Delta E_T \rangle_{a,u,d}$ as a function of temperature. As can be seen, the up and down values are not negligible but the average of the two, the "all" values,

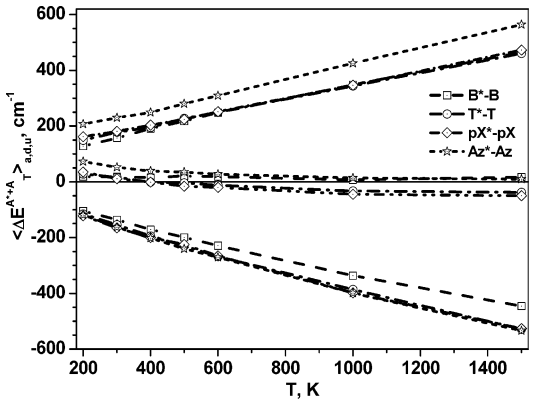

Figure 6. Up, down, and all values of average translational energy transferred $\langle \Delta E_T \rangle$ as a function of temperature. The excitation energy is 40700 cm^{-1} and the FOBS value is 0.35 cm^{-1} fs^{-1}.

are close to 0. Viewed with the information presented in paper 2 and in Figure 4, one can try to explain these results in the following way. In any individual trajectory there can be R and T energy lose or gain, but when tens of thousands of trajectories are averaged out, the overall contribution of rotation and translations is small and what we see, on the average, is mainly V−V transfer, as Figures 1 and 4 show. For that reason, of averaging up and down values, $\langle \Delta E \rangle_a$ is a meaningless quantity as far as shedding light on the mechanism of energy transfer. This explanation applies not only to self-collisions but also to mixed collisions of the title molecules reported in paper 2. What is left to explain is how can the values of $\langle \Delta E_R \rangle_{u,d}$ and $\langle \Delta E_T \rangle_{u,d}$ be so large, ∼400 and ∼500 cm^{-1} (at 1500 K), respectively, and the difference in the values of $\langle \Delta E_V \rangle_d$ between the hot and cold molecules be much smaller. The reason for that is efficient T−R and R−T energy interchange, with only the difference between $\langle \Delta E_R \rangle_{u,d}$ and $\langle \Delta E_T \rangle_{u,d}$ contributing to a little spill over to R/T−V.

Vibrational Temperature and Density of States. At constant excitation, the four molecules studied have different vibrational temperatures, T_V. B, being the smallest molecule, has the highest temperature and pX and AZ, being the largest, have the lowest, almost identical, vibrational temperature. This affects CET because the values of the various $\langle \Delta E \rangle$ are dependent on the vibrational temperature. To neutralize the effect of T_V, we have excited the title molecules in such a way that all have the same T_V, which we chose to be identical to the T_V (=2851 K) of B when excited to 40 700 cm^{-1}. Table 2 and Figure 7 give the CET values of the various $\langle \Delta E \rangle$'s. The larger molecules with higher excitations, but T_V's identical to the smaller ones, have higher values of $\langle \Delta E \rangle$ at all temperatures. So, molecules with identical T_V's do not have identical CET quantities. Not only that, pX and AZ with identical T_V's and excitation energies have significantly different CET quantities. This indicates that not only the values of the normal-mode frequencies are important but that internal rotations play a role in CET. From Table 2 it can be seen that replacing the collision partner in self-collision with B reduces the values of the various $\langle \Delta E \rangle$ in a significant way, which supports the discussion presented above that the small rigid B with high normal-mode frequencies is less efficient in CET than the larger molecules with lower normal-mode frequencies. Figure 7 also shows, in addition to the vibrational rotational energy loss of the hot molecule, $\langle \Delta E \rangle_{a,d}$, also the values of $\langle \Delta E_V \rangle_{a,d}$, the vibrational energy loss of the hot molecule. As can be seen, most of the energy loss is vibrational energy whereas rotational energy contributes very little to the energy loss at all temperatures.

TABLE 2: Energy Transfer Quantities of Self-Collisions and Excited Benzene, Toluene, *p*-Xylene and Azulene Colliding with Bath Benzene at 300 K[a]

	B*−B	T*−B	pX*−B	AZ*−B	T*−T	pX*−pX	AZ*−AZ
E'_V, cm^{-1}	41 069	53 777	66 597	66 897	53 777	66 597	66 897
$\langle\Delta E\rangle_a$	−755	−812	−930	−1241	−916	−1279	−1735
$\langle\Delta E\rangle_d$	−888	−959	−1093	−1413	−1051	−1440	−1907
$\langle\Delta E\rangle_u$	55	61	56	43	52	40	36
$\langle\Delta E_V\rangle_a$	−767	−827	−956	−1334	−930	−1304	−1767
$\langle\Delta E_V\rangle_d$	−874	−954	−1100	−1480	−1056	−1447	−1938
$\langle\Delta E_V\rangle_u$	27	48	37	36	46	30	30
$\langle\Delta E_R\rangle_a$	12	15	26	92	14	25	32
$\langle\Delta E_R\rangle_d$	−126	−115	−112	−50	−115	−117	−118
$\langle\Delta E_R\rangle_u$	144	134	142	157	133	152	164
$\langle\Delta E^{H+C_T}\rangle_a$	18	39	68	111	24	57	94
$\langle\Delta E^{H+C_T}\rangle_d$	−136	−147	−143	−142	−157	−150	−154
$\langle\Delta E^{H+C_T}\rangle_u$	157	199	228	285	186	235	278
$\langle\tau_{coll}\rangle_a$	2.23	2.33	2.28	2.32	2.52	2.77	3.25
$\langle\tau_{coll}\rangle_d$	2.39	2.49	2.43	2.44	2.69	2.93	3.43
$\langle\tau_{coll}\rangle_u$	1.29	1.34	1.36	1.39	1.34	1.40	1.46

[a] All excited molecules have the same vibrational temperature, T_V, of 2851 K, which is the T_V of benzene excited to 40 700 cm^{-1} plus the thermal energy of benzene at 300 K. The units of $\langle\Delta E\rangle$ are in cm^{-1} and the units of $\langle\tau_{coll}\rangle$ are in ps. $\langle\Delta E^{H+C_T}\rangle$ indicates the total translational energy gained or lost by the hot and cold molecules.

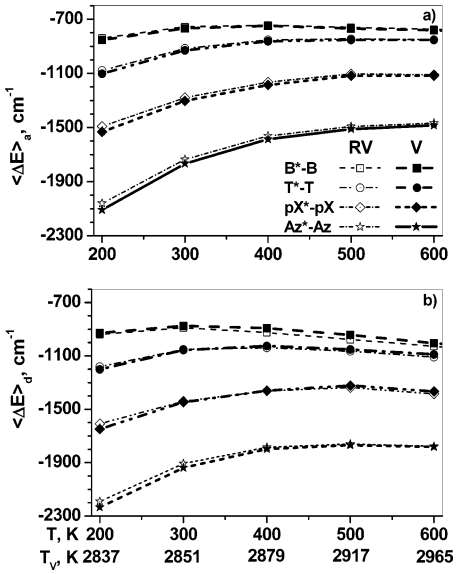

Figure 7. Absolute value of $\langle\Delta E\rangle$ as a function of the ambient temperature for constant vibrational temperature of $T_V = 2851$ K + thermal energy. RV indicates the internal vibrational/rotational energy and V the internal vibrational energy of the hot molecules. (a) is for all collisions and (b) is for down collisions. The excitation energy is 40700 cm^{-1} and the FOBS value is 0.35 cm^{-1} fs^{-1}.

Can the density of vibrational/rotational states, ρ(E), be correlated with the CET quantities reported in the tables and shown in Figures 1−7? We have calculated $\rho(E)$ for all molecules at excitation energy of 40 700 cm^{-1}, and as can be seen, there is no correlation between the CET quantities and $\rho(E)$. AZ is the most efficient collider but has a lower value of $\rho(E)$ than pX, and B, with the lowest value of $\rho(E)$ of the four molecules, is more efficient than T and pX at the high temperature range. Clearly dynamical effects dictate the process of CET.

Collision Complex Lifetimes. As indicated in the Theory, the collision lifetime is determined by the FOBS method in which a collision is defined by a change ϵ in the internal energy of the excited molecule in a time interval Δt at the beginning and at the end of the trajectory. The time between the beginning and end of the collision is determined by various factors: the intermolecular potential and the mass of the colliders. The heavier the colliders, the slower they move and the longer they remain in the vicinity of each other. Thus the AZ*−AZ pair is expected to have a longer lifetime than, e.g., B*−B. Figure 8 gives the value of $\langle\tau\rangle_d$ as a function of temperature for constant excitation energy. As can be seen, the heavier the colliders, the larger the value of $\langle\tau\rangle_d$. As the temperature increases, the value of $\langle\tau\rangle_d$ decreases and one would expect less chattering collisions and more impulsive ones.

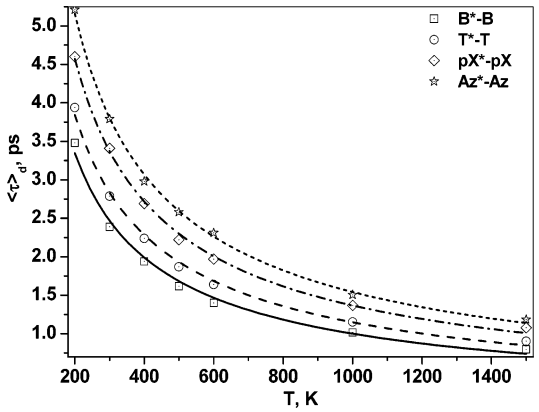

Figure 8. Average collision complex lifetimes of all down collisions as a function of temperature for constant excitation energy of 40 700 cm^{-1}. The FOBS value is 0.35 cm^{-1} fs^{-1}. The points are trajectory results and the lines are the fit of eq A6 to the data.

To understand better the nature of the collision complex, we use a simple model that shows the underlying factors that, taken together, explain the values of the collision lifetime. This model works because the actual energy-exchanging interaction time is much shorter than the collision time determined by FOBS. Therefore, the major part of τ is spent under the intermolecular potential without interference of the energy exchanging interactions. The details of the model are given in Appendix A. The model gives the length of the path the colliders travel within the collision complex and the dependence of $\langle\tau\rangle$ on the temperature. We use the model to determine the down-collision lifetimes. The temperature dependence of $\langle\tau\rangle_d$ is given by eq A6, $\langle\tau\rangle_d = \beta T^{-3/4}$, and the ratio for $\langle\tau\rangle_d$ of AZ at two different temperatures is $\langle\tau\rangle_d(200\text{ K})/\langle\tau\rangle_d(600\text{ K}) = (600/200)^{3/4} = 2.28$. The trajectory value is 2.42, a good agreement. Another example: $\langle\tau\rangle_d(300\text{ K})/\langle\tau\rangle_d(1500\text{ K}) = (1500/300)^{3/4} = 3.34$. The trajectory value is 3.21, not too bad either. Figure 8 shows also the fit to eq A6. As can be seen, a better agreement cannot be expected. The ratio of $\langle\tau\rangle_d$ for two different colliders, e.g., AZ and B, is given by eq A7.

$$\frac{\langle\tau\rangle_{d1}}{\langle\tau\rangle_{d2}} = \frac{(\sigma_{LJ})_1}{(\sigma_{LJ})_2}\left(\frac{(\mu\Omega^{(2,2)*})_1}{(\mu\Omega^{(2,2)*})_2}\right)^{1/2}\frac{1/x_1^{1/6} - 1}{1/x_2^{1/6} - 1}$$

At 200 K, the ratio is 1.55 and at 600 K the ratio is 1.59 whereas the trajectory values are 1.49 and 1.54, respectively, again in very good agreement with the model. The ratio of the β's in eq A6 for the two molecules taken from the best fit to the data is 1.54, in perfect agreement with the values reported above. What the model tells us is the heavier the collider the slower it moves and the distance it traverses is longer, both effects lead to greater interactions and large values of $\langle\Delta E\rangle$.

As indicated before, the longer the complex lives the higher is the value of $\langle\Delta E\rangle$. This can be seen in Figure 9a which shows $\langle\Delta E\rangle$ as a function of $\langle\tau\rangle$ at 200 K. There are many encounters

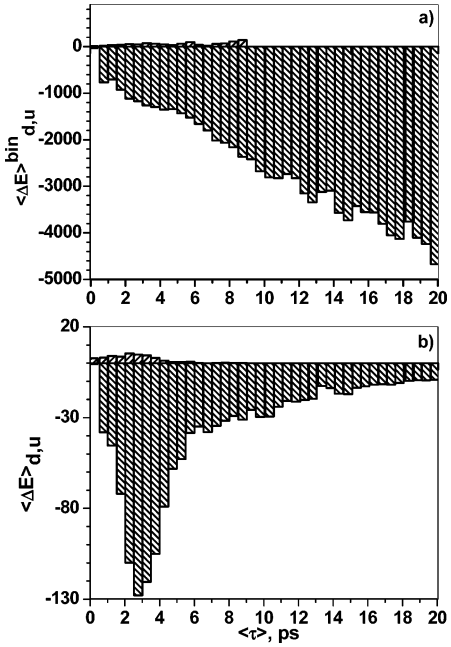

Figure 9. $\langle \Delta E \rangle$ as a function of the collision complex lifetime, $\langle \tau \rangle$, at 200 K for selfcollisions of azulene: (a) actual value; (b) weighted by the probability of having a given value of $\langle \tau \rangle$. The excitation energy is 40 700 cm^{-1}.

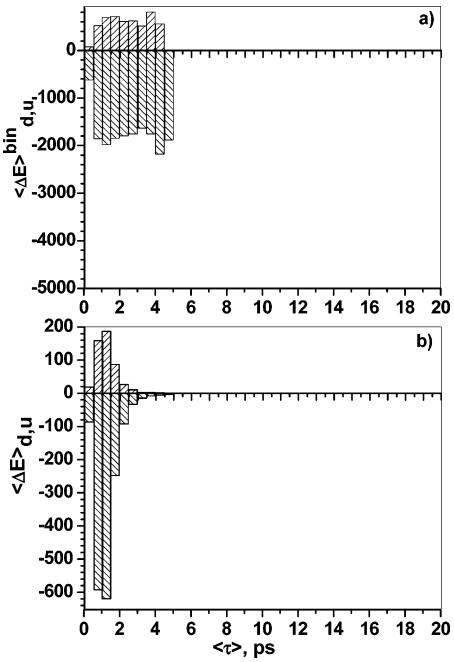

Figure 10. $\langle \Delta E \rangle$ as a function of the collision complex lifetime, $\langle \tau \rangle$, at 1500 K for selfcollisions of azulene: (a) actual value; (b) weighted by the probability of having a given value of $\langle \tau \rangle$. The excitation energy is 40 700 cm^{-1}.

in a chattering collision with long average lifetime. The actual contribution to CET at each $\langle \tau \rangle$ is given in Figure 9b where the results of (a) are multiplied by the probability of having a given $\langle \tau \rangle$ at a given temperature. The maximum of the contribution is at 2.5 ps, but there is a long tail at much longer lifetimes. As shown in Figure 10, the situation changes at high temperatures. At 1500 K $\langle \Delta E \rangle$ does not depend on $\langle \tau \rangle$ and there are almost no long-lived collisions, which mean that the collisions are more impulsive and CET is a short duration event. This time dependent behavior at low temperatures is absent in collisions with a monatomic bath. As discussed in paper 2, the actual

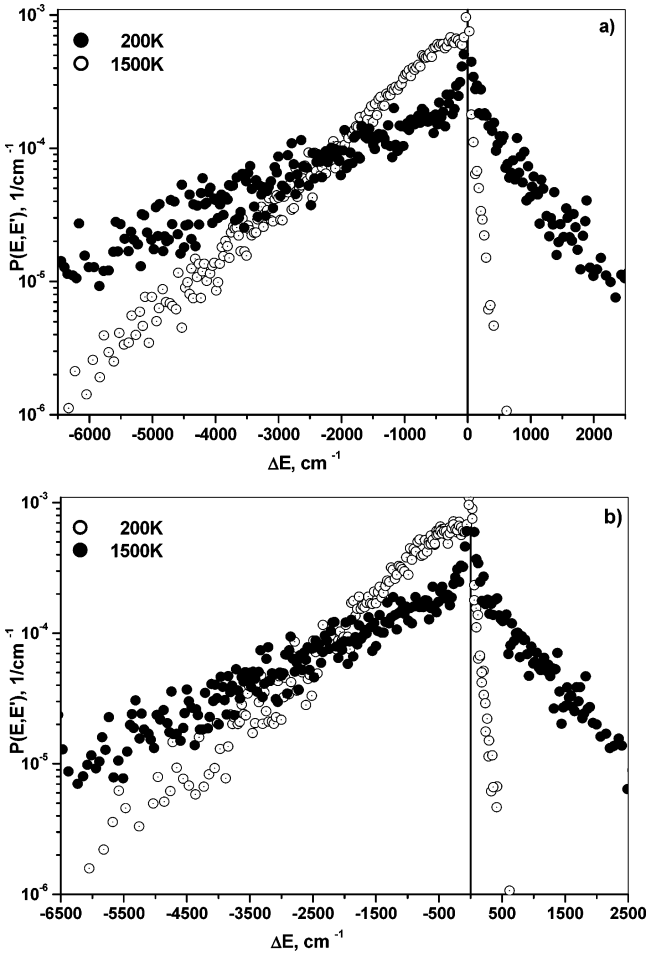

Figure 11. Collisional energy transfer probability density function, $P(E,E')$, vs ΔE for self-collisions of (a) benzene*−benzene and (b) toluene*−toluene at 200 K (empty symbols) and 1500 K (full symbols). Note the change in the shape of the two lines. The excitation energy is 40 700 cm^{-1}. There is a noticeable supercollision tail at high temperatures at the down-collision part.

energy transfer event lasts 30−40 fs, regardless of how long the monatomic gas hovers in the vicinity of the donor.

Collisional Energy Transfer Probability Density Function. The values of $\langle \Delta E \rangle$ are important quantities that give an indication of the relative efficiency of various colliders and excited molecules. However, the important quantity in energy transfer is $P(E,E')$. With $P(E,E')$ known, it is possible to solve the master equation and obtain rate coefficients and energy transfer quantities. Unfortunately, experimental data are scarce. The KCSI method of Luther, Lenzer and co-workers[17,18] is an important step in elucidating the details of CET but it uses a master equation to obtain $P(E,E')$. The diode laser experiments of Flynn, Mullin and co-workers[19−23] provide important mechanistic information, but they give only the supercollision tail of the distribution. The only experimental work that claims to give directly the whole distribution function is that of Ni and co-workers who studied energy transfer in the AZ*−Kr system in a crossed molecular beam.[24] Computational work fare only a little better. Trajectory calculations give unnormalized $P(E,E')$ as a routine matter,[25−27] because each trajectory gives ΔE_u or ΔE_d directly. The normalization, however, depends on the chosen value of b_m, which is hard to pin down exactly. The unnormalized $P(E,E')$ provides ample information as to the shape and the supercollision[28−30] tail of the distribution. Figures 11 and 12 show $P(E,E')$ for B*−B, T*−T, pX*−pX, and AZ*−AZ collisions at two temperatures. At 200 K the down-collision

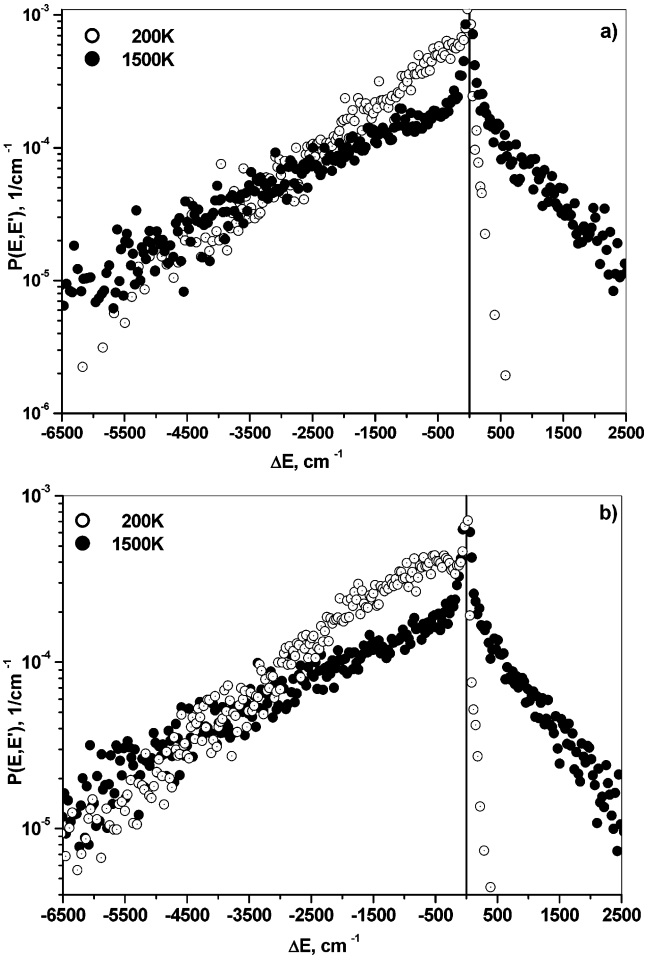

Figure 12. Collisional energy transfer probability density function, $P(E,E')$, vs ΔE for self-collisions of (a) *p*-xylene*−*p*-xylene and (b) azulene*−azulene at 200 K (empty symbols) and 1500 K (full symbols). Note the change in the shape of the two lines. The excitation energy is 40 700 cm^{-1}. There is a noticeable supercollision tail at high temperatures at the down-collision part.

wing of the distribution is convex and at 1500 K it is concave. In a series of runs, not shown here, $P(E,E')$ was plotted at various temperatures and it was found that the higher the temperature, the more concave is the down-collision wing of the distribution and the larger is the supercollision[28−30] tail of the distribution. As shown in paper 2, in Ar−polyatomic collisions, in contrast, $P(E,E')$ is always concave and can be fitted with a double exponential function, It is interesting to note that our results for AZ−Ar collisions depicted in Figure 13 agree qualitatively very well with those of Ni and coworkers.[24]

Supercollision. Very high energy collisions, supercollisions,[28−30] SC, are defined as collisions that transfer inordinately large amounts of energy. They were found experimentally and in trajectory calculations between excited polyatomic molecules and monatomic bath[31−37] and in trajectory calculations of aromatic polyatomic−polyatomic collisions.[3,4] Previously,[31,36] they were defined as those that transfer $\Delta E_d > 5\langle\Delta E_d\rangle$ and because $\langle\Delta E_d\rangle$ depends on the temperature, the SC threshold is temperature dependent. Thus, from Figures 11 and 12 it can be seen that SC occur above different values of ΔE for each of the collision pairs. At 200 K, for B*−B and T*−T collisions, it occurs when $\Delta E_d > 5000$ cm^{-1}, for pX*−pX above 6500 cm^{-1} and for AZ*−AZ above 7500 cm^{-1}. The $\Delta E_d > 5\langle\Delta E_d\rangle$ rule need not be taken too seriously because it does not have

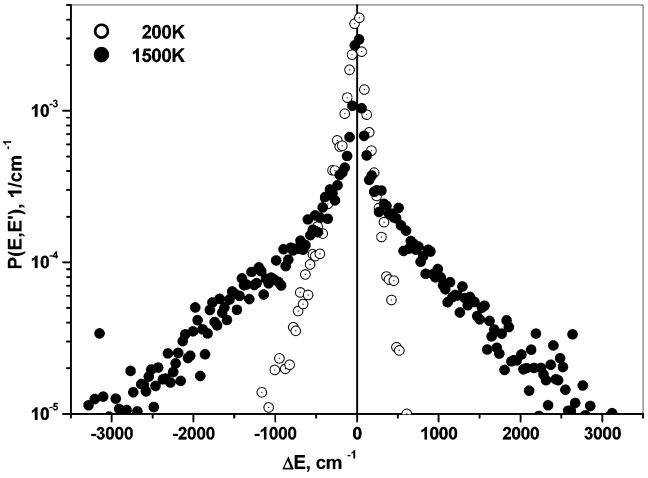

Figure 13. Collisional energy transfer probability density function, $P(E,E')$, vs ΔE for collisions of azulene*−Ar at 200 K (empty symbols) and 1500 K (full symbols). The excitation energy is 40 700 cm^{-1}. There is a noticeable supercollision tail at high temperatures at the down-collision part.

TABLE 3: Density of States, $\rho(E)$, of the Four Molecules at an Excitation Energy of 40 700 cm^{-1}

molecule	comments	$\rho(E)$
B		1.5×10^{15}
T	free rotor	9.1×10^{19}
	hindered rotor	3.5×10^{19}
pX	free rotors	1.0×10^{24}
	hhindered rotor	5.8×10^{23}
AZ		2.7×10^{22}

any theoretical basis. For all we know, it can be $\Delta E_d > 4\langle\Delta E_d\rangle$ or any other reasonable option. The fact is a very large amount of energy is transferred in a single collision. This fact is of great importance in chemical kinetics because small amounts of SC go a long way in increasing the values of the rate coefficients of chemical reactions.[25]

Comparison with Experiments. Experiments in energy transfer between an excited polyatomic molecule and a cold bath molecule are hard to perform, and therefore, hard to come by. The problem is discussed in a paper by Lenzer and Luther[2] and additional examples for self-collisions are given below. Lenzer and Luther[2] compared results for energy transfer in azulene−Ar and azulene−CO_2 obtained by three methods, Barker's IR fluorescence,[37−41] Troe's UV absorption,[42−44] and Lenzer and Luther kinetically controlled selective ionization.[17,18] Lenzer and Luther[2] show that major discrepancy in the results can be removed by minor changes in parameters of the equations that are used to interpret the results, especially in the contribution of self-collisions and in the calibration curves used to interpret the results. Results for self-collisions of T and pX by Troe's group,[47,48] given in Table 4, show that the results vary depending on the method used for interpreting the results. The uncertainties in the experimental results and the uncertainties in the intermolecular potential used in the trajectory calculations not withstanding, it is worthwhile, nevertheless, to compare the experimental and computational results. To compare the results, the trajectory data need to be converted to a format that uses the same parameters that are used to interpret the experimental results. We do so with the help of eq 2 in the Theory and the results of the comparison are given in Table 4. As can be seen, the agreement is good. The trend $\langle\Delta E\rangle(B) \approx \langle\Delta E\rangle(T) < \langle\Delta E\rangle(pX)$ is the same in experiment and in computation. The latter differ from the former values by only 12−20%, a very acceptable result. The agreement is even better when one

TABLE 4: Energy Transfer Quantities of the Excited Molecule at Various Temperatures Normalized to Experimental Quantities According to Eq 3[a]

system	E_{excit}, cm^{-1}	$\langle E \rangle$	$-\langle \Delta E \rangle$	$-\langle \Delta E \rangle_d$	ref	$-\langle \Delta E \rangle_{traj}$	$-\langle \Delta E \rangle_{d,traj}$
B−B	40 000	25 000	869	1477	40	1114	1671
T−T	40 000	25 000	880		45	1066	
	38 100	24 000	650		46		
	40 800		867		46		
	53 700		710		47		
	53 700		780		47		
	53 700		770		48		
pX−pX	40 000	25 000	1080		45	1315	
	53 700		1040		47		
	53 700		1250		47		
	53 700		1000		48		
AZ−AZ	40 700		1700		37	1490	

[a] $E_v = 40\,700\ cm^{-1}$ + thermal energy, FOBS = $0.35\ cm^{-1}\ fs^{-1}$.

considers that the values of $\langle \Delta E \rangle$ go up with excitation energy and that the internal energy in most experiments is 25 000 cm^{-1} compared with 40 700 cm^{-1} in the present trajectory calculations. Bae et al.[45] who studied self-collisions in T and in pX, among other molecules, make a linear correlation between the values of $\langle \Delta E \rangle$ and the number of modes in T, pX and mesitylene (trimethylbenzene). This may apply to substituted benzene but is surely not a general rule, because in self-collision of AZ, with the same number of modes as pX, the values of $\langle \Delta E \rangle$ are much larger than that of pX. It also varies with temperature in a complicated way, as discussed above, and this rule will lose its applicability at temperatures not studied in the experiments. Ian Smith and co-workers[46] have studied T collisions and their results agree with those of Bae et al. Troe and co-workers[47,48] have studied energy transfer in substituted benzenes, among them T and pX, by following the quenching of photodissociation. Their results are also given in Table 4 and support the trend reported in this work.

Summary. What can be learned about collisional energy transfer from the present and the previously published two papers in the series[3,4] that deal with energy transfer in intercollisions between small aromatic compounds: benzene, toluene, *p*-xylene (*p*-dimethylbenzene), and azulene and all those with Ar? First and foremost is: every molecule behaves somewhat differently and even in a set of similar molecules it is very hard to predict, let alone quantify, simple propensity rules that will guide future exploration of additional molecules. Nevertheless, some important conclusions emerge from the present series of studies and they are listed below. The second generalization is the mechanism of energy transfer in polyatomic−polyatomic collisions is different than that in aromatic polyatomic−monatomic collisions even though there are some common features between the two types of collisions. The specific features of aromatic polyatomic−polyatomic collisions are:

(a) The major channel for energy transfer in aromatic polyatomic−polyatomic collisions is vibration to vibration, V−V, transfer whereas in polyatomic−monatomic collisions it is vibration, rotation to translation, V/R−T.

(b) Rotational and translational, V/R−T, energy transfer are minor, but important, channels in energy transfer and assist in the V−V transfer. Very small net overall rotational energy, $\langle \Delta E_R \rangle_a$, and translational energy, $\langle \Delta E_T \rangle_a$, is transferred during the collision but the average values of the up and down energy transferred, $\langle \Delta E_R \rangle_{u,d}$ and $\langle \Delta E_T \rangle_{u,d}$ are fairly large, which indicate active participation of rotation and translation in the energy transfer process.

(c) There is large R−T and T−R energy exchange with minor effects on the vibrational energy of the hot molecule.

(d) The gateway mode for energy transfer is the lowest lying out-of-plane mode of the aromatic molecules studied.

(e) Freezing rotations enhance energy transfer in aromatic polyatomic−polyatomic collisions and hinder it in polyatomic−monatomic collisions.

(f) Internal rotations in the excited molecule hinder energy exchange whereas in the bath molecule at low temperatures they do not because the internal rotors are not excited. Thus, azulene with the same number of normal modes as *p*-xylene but without internal rotations is much more efficient in transferring energy to benzene bath molecules.

(g) Energy transfer at low and high temperatures is more efficient than at intermediate temperatures.

(h) The temperature dependence of $\langle \Delta E \rangle$ is complex and cannot be given by simple exponent.

(i) Low-frequency modes enhance energy transfer. Thus, azulene with modes of lower frequencies than benzene is much more efficient in transferring energy.

(j) Vibrational temperatures affect energy transfer. In a series of aromatic polyatomic molecules of different sizes and identical vibrational temperatures, the largest values of $\langle \Delta E \rangle$ occur in the largest molecules with the lowest frequency modes.

(k) The value of $\langle \Delta E \rangle$ in aromatic polyatomic−polyatomic collisions is much larger than that in a polyatomic−monatomic collisions due to the fact that there is an extra V−V channel that is absent in the latter.

(l) The down-collisions wing of the energy transfer probability density function, $P(E,E')$ in aromatic polyatomic−polyatomic collisions is convex at low temperatures and becomes concave at higher temperatures. The shape of down-collisions wing of $P(E,E')$ in polyatomic−monatomic collisions is concave at moderate and high temperatures.

(m) The down-collisions wing of $P(E,E')$ has a noticeable supercollision tail.

(n) In aromatic polyatomic−polyatomic collisions, the collision lifetimes affect the values of ΔE inasmuch as at low temperatures chattering collisions containing multiple encounters occur, each encounter transferring a given amount of vibrational energy to the cold polyatomic bath. The collision complex lifetime has no effect on the value of ΔE in polyatomic−monatomic collisions because the actual energy transfer event occurs in the last few tens of femtoseconds of the collision complex lifetime. How long the atom hovers over the polyatomic molecule has no effect on the final outcome.

(o) The relative values of $\langle \Delta E \rangle_d$ in self-collisions of benzene, toluene, *p*-xylene, and azulene change with temperature. That is to say, *p*-xylene is more efficient than benzene at low temperatures and less efficient at high temperatures.

(p) Agreement between experiments and present computations is good.

(q) There is no correlation between the density of vibrational/rotational states of the excited molecules and energy transfer quantities.

Quo Vadis. Collisional energy transfer is of major importance in understanding and interpreting chemical reaction in the gas phase. Nevertheless, our understanding of the major features of energy transfer are sketchy and important details are lacking. Unlike RRKM theory, with its basic concept of statistical redistribution of energy in the excited molecule, there is no one simple underlying concept that governs intermolecular energy transfer in large aromatic polyatomic molecules and possibly in other types of polyatomic−polyatomic collisions. There are known bits and pieces that are part of a puzzle not yet solved. Molecules exchange energy differently when they are hot and

when they are cold, or at high and at low temperatures. In a given system with a set of given initial conditions there are various energy transfer mechanisms operating simultaneously, possibly one for low values of ΔE, one for large values of ΔE, and one for supercollisions. The present computational work, together with that presented in papers 1 and 2, deals with four aromatic compounds and exposed a rich and complex energy transfer behavior. This work, together with previous trajectory calculations, compares favorably with the available experimental data. The experience gained is: trajectory results are reliable and shed light on important features of energy transfer. The confidence thus gained should be used to expend and perform *systematic* studies on other systems not studied experimentally. On the experimental side, finding new approaches to evaluate $P(E',E)$ is of prime importance. The beam experiments of Ni and the KCSI method of Luther and Lenzer should be compared and new experimental approaches explored. Whatever the future may bring, one thing is clear. Intermolecular energy transfer is controlled by complex and diverse mechanisms and cannot be explained, unlike RRKM, by one overriding concept or one simple model.

Acknowledgment. This work is supported by the Ministry of Science and the Arts under the KAMEA program.

Appendix A

The Lennard-Jones, LJ, potential is given by the expression

$$V = 4\epsilon_{LJ}[(\sigma_{LJ}/r)^{12} - (\sigma_{LJ}/r)^{6}] \qquad \text{(A1)}$$

Figure A1 shows the LJ potential for B*−B and AZ*−AZ collisions. As can be seen, the distance between σ_{LJ}(B) and a given potential, V_α, is smaller than the distance σ_{LJ}(AZ) and V_α.

If we assume that the beginning of a collision, as defined by FOBS, takes place at potential energy V_α, then solving for r at V_α, r_α, one obtains, after correction for the collision integral $\Omega^{(2,2)*}$:

$$r_\sigma = \sigma_{LJ}[\Omega^{(2,2)*}]^{1/2}/x^{1/6} \qquad \text{(A2)}$$

where x is given by

$$x = -(1 - (1 + V_\alpha/\epsilon_{LJ})^{1/2})/2 \qquad \text{(A3)}$$

The distance the molecule travels is twice the distance between r_α and σ. The distance each way is

$$l = r_\alpha - \sigma = \sigma_{LJ}[\Omega^{(2,2)*}]^{1/2}(1/x^{1/6} - 1) \qquad \text{(A4)}$$

The temperature dependence of $\Omega^{(2,2)*}$ is[15] $T^{-0.5}$. The value of $\langle\tau\rangle_d$ is given by

$$\langle\tau\rangle_d = 2l/\upsilon \qquad \text{(A5)}$$

υ is the average speed of the molecules $(8kT/\pi\mu)^{1/2}$. Lumping all the temperature independent parameters into one constant, β one obtains the temperature dependence

$$\langle\tau\rangle_d = \beta T^{-3/4} \qquad \text{(A6)}$$

To compare the values of $\langle\tau\rangle_d$ of two different colliders, one uses eqs A2−A5 and divides the expressions for two different colliders

$$\frac{\langle\tau\rangle_{d1}}{\langle\tau\rangle_{d2}} = \frac{(\sigma_{LJ})_1}{(\sigma_{LJ})_2}\left(\frac{(\mu\Omega^{(2,2)*})_1}{(\mu\Omega^{(2,2)*})_2}\right)^{1/2}\frac{1/x_1^{1/6} - 1}{1/x_2^{1/6} - 1} \qquad \text{(A7)}$$

Subscripts 1 and 2 indicate two different colliders.

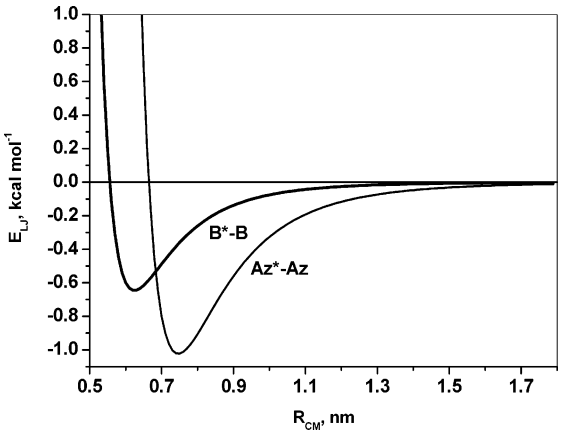

Figure A1. Lennard-Jones intermolecular potential vs center-of-mass distance for benzene*−benzene and azulene*−azulene collisions. For the same intermolecular interaction energy, E_{LJ}, the azulene pair travels a longer distance than the benzene one.

References and Notes

(1) Oref, I.; Tardy, D. C. *Chem. Rev.* **1990**, *90*, 1407.
(2) Lenzer, T.; Luther, K. *Phys. Chem. Chem. Phys.* **2004**, *6*, 955.
(3) Bernshtein, V.; Oref, I. *J. Phys. Chem. B* **2005**, *109*, 8310.
(4) Bernshtein, V.; Oref, I. *J. Phys. Chem.*, in press.
(5) Clary, D. C.; Gilbert, R. G.; Bernshtein, V.; Oref, I. *FaradayDiscuss.* **1995**, *102*, 423.
(6) Bernshtein, V.; Oref, I. *J. Chem. Phys.* **1997**, *106*, 7080.
(7) Draeger, J. A. *Spectrochim. Acta* **1985**, *41A*, 607.
(8) Lim, K. F.; Gilbert, R. G. *J. Phys. Chem.* **1990**, *94*, 77.
(9) Lim, K. F. *J. Chem. Phys*. **1994**, *100*, 7385.
(10) Lim, K. F. Program SIGMON: An Aid for the Semiempirical Fitting of the Intermolecular Potential, School of Biological and Chemical Sciences, Deakin University, Geelong, VIC 3217, Australia, 1992.
(11) Hase W. L.; Duchovic R. J.; Hu X.; Komornicki, A.; Lim, K. F.; Lu D.-H.; Peslherbe, G. H.; Swamy, K. N.; Vande-Linde, S. R.; Varandas, A.; Wang, H.; Rolf R. J. Venus, Quantum Chemistry Program Exchange. *QCPE Bull.* **1996**, *16* (4), 43 [QCPE Program 671].
(12) Nakashima, N.; Yoshihara, K. *J. Chem. Phys.* **1983**, *79*, 2727.
(13) Bernshtein, V.; Oref, I. *J. Phys Chem. A* **2000**, *104*, 706.
(14) (a) Reid, R. C.; Sherwood, T. K. *The Properties of Gases and Liquids*, 2nd ed.; McGraw-Hill: New York, 1966. b). Troe, J. *J. Chem. Phys.* **1977**, *66*, 4758.
(15) Kim, S. K.; Ross, J. *J. Chem. Phys*. **1967**, *46*, 818.
(16) Clarke, D. L.; Oref, I.; Gilbert, R. G.; Lim, K. F. *J. Chem. Phys.* **1992**, *96*, 5983.
(17) Lenzer, T.; Luther, K.; Reihs, K.; Symonds, A. C. *J. Chem. Phys.* **2000**, *112*, 4090.
(18) Hold, U.; T. Lenzer, T.; Luther, K.; Reihs, K.; Symonds, A. C. *J. Chem. Phys.* **2000**, *112*, 4076.
(19) E. T. Sevy, S. M. Rubin, Z. Lin, G. W. Flynn, J. *Chem. Phys.* **2000** *113*, 4912.
(20) Michaels, C. A.; Lin, Z.; Mullin, A. S.; Tapalian, H. C.; Flynn, G. W. *J. Chem. Phys*. **1997**, *106*, 7055.
(21) Michaels, C. A.; Flynn, G. W. J. *Chem. Phys.* **1997**, *106*, 3558.
(22) Park, J.; Li, Z. M.; Lemoff, A. S.; Rossi, C.; Elioff, M. S.; Mullin, A. S. *J. Phys. Chem*. **2002**, *106*, 3642.
(23) Wall, M. C.; Mullin, A. S. *J. Chem. Phys.* **1998** *108*, 9658.
(24) Liu, C. L.; Hsu, H. C.; Lyu, J. J.; Ni, C. K. *J. Chem. Phys.* **2005**, *123*, 131102.
(25) Bernshtein, V.; Oref, I.; Lendvay, G. *J. Phys. Chem.* **1996**, *100*, 9738.
(26) Bernshtein, V.; Oref, I. *J. Chem. Phys.* **1998**, *108*, 3543.
(27) Higgins, C. J.; Chapman, S. *J. Phys. Chem. A.* **2004**, *108*, 8009.
(28) Hassoon, S.; Oref, I.; Steel, C. J. *Chem. Phys.* **1988**, *89*, 1743.

(29) Morgulis, L. M.; Sapers, S. S.; Steel, C.; Oref, I. *J. Chem. Phys*. **1989**, *90*, 923.
(30) Pashutzki, A.; Oref, I. *J. Phys. Chem*. **1988**, *92*, 178.
(31) Clarke, D. L.; Thompson, K. C.; Gilbert, R. G. *Chem. Phys. Lett*. **1991**, *182*, 357.
(32) Oref, I. *Chem. Phys.* **1994**, *187*, 163.
(33) Clary, D. C.; Gilbert, R. G.; Bernshtein, V.; Oref, I. *Faraday Discuss*. **1995**, *102*, 423.
(34) Bernshtein, V.; Oref, I. *J. Chem. Phys.* **1997**, *106*, 7080.
(35) Bernshtein, V.; Oref, I. *J. Chem. Phys.* **1998**, *108*, 3543.
(36) Oref, I. Supercollisions. In *Energy Transfer from Large Molecules in Nonreactive Systems*; Barker, J. R., Ed.; Advances in Chemical Kinetics and Dynamics Series, Vol. 2B; JAI Press: London, 1995; pp 285−298.
(37) Shi, J.; Barker, J. R. *J. Chem. Phys.* **1988**, *88*, 6219.
(38) Rossi M. J.; Pladziewicz J. R.; Barker, J. R. *J. Chem. Phys.* **1983**, *78*, 6695.
(39) Yerram, M. L.; Brenner, J. D.; King, K. D.; Barker, J. R. *J. Phys. Chem*. **1990**, *94*, 6341.
(40) Toselli, B. M.; Barker, J. R. *J. Chem. Phys.* **1991**, *95*, 8108; **1992**, *97*, 1809.
(41) Barker, J. R.; Brenner, J. D.; Toselli, B. M. *Adv. Chem. Kinet. Dynam*. **1995**, *2b*, 393.
(42) Damm, M.; Hippler, H.; Olschewski, H. A.; Troe, J.; Wilner, J. *Z. Phys. Chem. (Munich*) **1990**, *166*, 129.
(43) Damm, M.; Deckert, F.; Hippler, H.; Troe, J. J. *Phys. Chem.* **1991**, *95*, 2005.
(44) Damm, M.; Deckert, F.; Hippler, H. *Ber. Bunzen-Ges.* **1997**, *101*, 1901.
(45) Bea, S. Y.; Lee I. J. Park J. *Chem. Phys.* **2000**, *103*, 255.
(46) Wright, S. M. A.; Sims, I. R.; Smith, I. W. M. *J. Phys. Chem. A* **2000**, *104*, 10347.
(47) Brand, U.; Hippler, H.; Lindemann, L.; Troe, J. *J. Phys. Chem.* **1990**, *94*, 6305.
(48) Hippler, H.; Troe, J.; Wendelken, H. J. *J. Chem. Phys.* **1983**, *78*, 6709, 6718.